

Multimodal Adaptation of CLIP for Few-Shot Action Recognition

Jiazheng Xing¹, Mengmeng Wang¹, Xiaojun Hou¹, Guang Dai², Jingdong Wang³, Yong Liu^{1*}

¹ Zhejiang University, ² SGIT AI Lab, ³ Baidu Inc.

{jiazhengxing, mengmengwang, xiaojunhou}@zju.edu.cn

yongliu@iipc.zju.edu.cn, guang.gdai@gmail.com, wangjingdong@baidu.com

Abstract

Applying large-scale pre-trained visual models like CLIP to few-shot action recognition tasks can benefit performance and efficiency. Utilizing the “pre-training, fine-tuning” paradigm makes it possible to avoid training a network from scratch, which can be time-consuming and resource-intensive. However, this method has two drawbacks. First, limited labeled samples for few-shot action recognition necessitate minimizing the number of tunable parameters to mitigate over-fitting, also leading to inadequate fine-tuning that increases resource consumption and may disrupt the generalized representation of models. Second, the video’s extra-temporal dimension challenges few-shot recognition’s effective temporal modeling, while pre-trained visual models are usually image models. This paper proposes a novel method called Multimodal Adaptation of CLIP (MA-CLIP) to address these issues. It adapts CLIP for few-shot action recognition by adding lightweight adapters, which can minimize the number of learnable parameters and enable the model to transfer across different tasks quickly. The adapters we design can combine information from video-text multimodal sources for task-oriented spatiotemporal modeling, which is fast, efficient, and has low training costs. Additionally, based on the attention mechanism, we design a text-guided prototype construction module that can fully utilize video-text information to enhance the representation of video prototypes. Our MA-CLIP is plug-and-play, which can be used in any different few-shot action recognition temporal alignment metric.

1. Introduction

Few-shot action recognition aims to quickly learn new action categories using limited labeled samples. Compared with general action recognition, the main distinction of few-shot action recognition lies in the extremely small amount of labeled data in each task and the variety of task types.

*Corresponding authors.

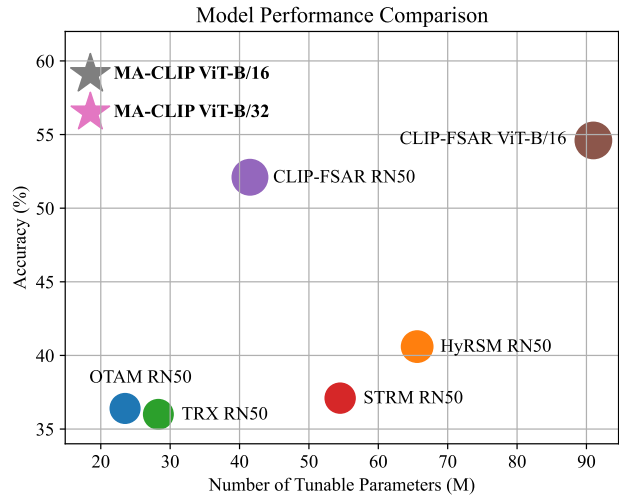


Figure 1. Performance comparison of different few-shot action recognition methods under the 5-way 1-shot settings on the SSv2-Small dataset, including our MA-CLIP, OTAM [3], TRX [33], STRM [38], HyRSM [46], and CLIP-FSAR [44]. Bubble or star size indicates the recognition accuracy. Our MA-CLIP achieves the highest recognition accuracy with the least number of tunable parameters.

Therefore, few-shot action recognition requires models to possess the ability to quickly transfer between different tasks, making this work extremely difficult. Previous methods [3, 61, 56, 33, 38, 49, 46, 22, 14] mainly used metric-based framework and episode training to solve the transfer to new classes. However, despite the short training time for each task, it requires a large amount of training on similar tasks to enable the model to have strong generalization capabilities across various tasks. Therefore, relying solely on the above solutions still requires the model to spend much time training on different datasets, which somewhat hinders its application in industry.

With the development of computer vision, more and more large foundation visual models [34, 54, 43, 39, 15, 19] have emerged. Their key to these models is providing an excellent pre-trained model, which can be fine-tuned for

downstream tasks to provide strong transferability. By utilizing large foundation models such as CLIP for downstream tasks such as action recognition [42, 30], segmentation [35, 28, 50], object detection [10, 58], et al., the “pre-training, fine-tuning” paradigm leverages the power of robust pre-trained models, thus eliminating the need to train a network from scratch and obtaining impressive performance. Due to the powerful generalization ability of the CLIP pre-trained model, applying it to few-shot action recognition tasks can significantly reduce the number of similar training tasks during the fine-tuning stage to save training time. Furthermore, CLIP is a multimodal model, and for few-shot action recognition tasks with limited visual samples, introducing the additional textual features can serve as a powerful aid. CLIP-FSAR [44] follows this approach using CLIP [34] and has achieved good results. However, this method has at least two drawbacks. First, each task has limited trainable labeled samples for few-shot action recognition, so it is necessary to minimize the number of training parameters as much as possible to avoid the overfitting phenomenon. Insufficient complete fine-tuning will increase the consumption of computational resources and time and may disrupt the good generalized representation of the foundation models. Second, large foundation models are mostly image pre-trained models, while videos have an extra-temporal dimension compared to images. One of the challenges in few-shot recognition is how to perform temporal modeling effectively. We applied CLIP to perform zero-shot action recognition and found that while it performed well on spatial datasets, its performance was not ideal on temporal datasets, highlighting the importance of temporal modeling. CLIP-FSAR only uses an additional temporal module to extend the image model, which cannot fully integrate temporal information in videos.

To overcome the above drawbacks, we followed a new approach called parameter-efficient fine-tuning, i.e., PEFT, that efficiently utilizes large foundation models. PEFT was initially applied in natural language processing (NLP) [12, 21, 55, 13] and has made remarkable progress in computer vision (CV) [1, 17, 16, 51, 47] in recent years. The core idea is to keep the large pre-trained foundation model frozen to achieve robust performance while only fine-tuning a small number of extra parameters. This idea is very well-suited for few-shot action recognition, which can minimize the number of learnable parameters and enable the model to possess the ability to transfer across different tasks quickly. In addition, our task involves video understanding, while most large foundation models are based on images lacking temporal understanding. To address this issue, adding a small number of trainable parameters for temporal modeling in the large foundation model proves effective, such as AIM [51] and Vita-CLIP [47].

Based on these findings, we propose a novel method for

few-shot action recognition, dubbed **MA-CLIP**, a shot for **Multimodal Adaptation of CLIP**. Specifically, we adopt the idea of PEFT and choose CLIP [34] as our baseline due to its multimodal capability. We freeze CLIP’s pre-trained image and text encoders during fine-tuning and add some lightweight adapters [12, 51] and tunable parameters. As CLIP is a foundation model for image-text pairs, the adapters we design can combine the bi-modal information of the videos (spatiotemporal information) and texts (semantic information) for task-oriented modeling. Meanwhile, we design a text-guided prototype construction module based on the attention mechanism to fully utilize the video-text multimodal information and enhance the representation of video class prototypes. Finally, our MA-CLIP is plug-and-play and can be used in any different few-shot action recognition temporal alignment metric, i.e., video matcher. Extensive experiments unequivocally demonstrate that our method attains exceptional performance while employing the fewest tunable parameters, as depicted in Fig. 1.

In summary, we make the following contributions:

- We propose a novel method to adapt CLIP for few-shot action recognition by adding lightweight adapters and relatively few tunable parameters. The adapters we designed can combine information from video-text multimodal sources for task-oriented modeling, which is fast, efficient, and has low training costs.
- Based on the attention mechanism, we design a text-guided prototype construction module that can fully utilize video-text information to further enhance the representation of video prototypes.
- Our plug-and-play method can be used in any different few-shot action recognition temporal alignment metric. Experiments demonstrate that our method performs excellently using any metric in various task settings.
- Extensive experiments on five widely used datasets have shown that our method can achieve outstanding performance with minor trainable parameters.

2. Related Works

2.1. Few-shot Learning

Few-shot learning leverages the episodic training paradigm, wherein a limited number of labeled training samples from a large number of related tasks are utilized to effectively represent a substantial volume of labeled training samples. In recent years, research on few-shot learning can be mainly classified into adaptation-based and metric-based methods. The former [8, 31, 26] aims to find a network initialization that can be fine-tuned for unknown tasks using limited labeled data, called *gradient by gradient*. The

latter [36, 40, 53, 52, 6, 23] aims to acquire knowledge of feature space and compare task features using various matching strategies, referred to as *learning to compare*.

2.2. Few-shot Action Recognition

The core concept of few-shot action recognition is akin to few-shot learning, but including the temporal dimension amplifies the problem’s difficulty. Despite the potential benefits of adaptation-based methods (e.g., MetaUVFS [32]), these approaches have received limited attention in few-shot action recognition due to their high computational requirements and extensive experimental time. Instead, existing research predominantly emphasizes metric-based learning approaches with varying focuses. On the one hand, some methods focus on class prototype matching strategies. TRX [33] matches each query sub-sequence with all sub-sequences in the support set, facilitating correspondences between different videos. OTAM [3] introduces a temporal alignment module to calculate the distance value between query and support set videos. On the other hand, some approaches aim to enhance feature representation. For instance, SloshNet [49] leverages a feature fusion architecture search module to exploit low-level spatial features, combining it with long-term and short-term temporal modeling modules to encode complementary global and local temporal representations. STRM [38] adopts local and global enrichment modules for spatiotemporal modeling, while HyRSM [46] utilizes hybrid relation modeling to learn task-specific embeddings. With the development of large foundation visual models, how to apply them in downstream tasks is receiving increasing attention. CLIP-FSAR [44] makes attempts using the CLIP pre-trained model and designs a video-text contrastive objective and a prototype modulation, achieving good results. However, completely fine-tuning the visual encoder would increase computational costs and risk catastrophic forgetting. Additionally, CLIP is an image pre-trained model that CLIP-FSAR does not extend the visual encoder for temporal modeling. Our approach will address the problems encountered in the CLIP-FSAR mentioned above.

2.3. Parameter-efficient Fine-tuning (PEFT) for Vision Models

With the development of an increasing number of large-scale visual foundational models [34, 54, 43, 39, 15, 19], more and more attention is focused on parameter-efficient fine-tuning, i.e., PEFT. PEFT, initially employed in natural language processing (NLP) [12, 21, 55, 13], has exhibited impressive advancements in computer vision (CV) in recent times. The fundamental concept revolves around preserving the immutability of the extensive pre-trained models to ensure consistent and reliable performance, focusing solely on refining a limited set of additional parameters.

The application of PEFT in computer vision can be broadly categorized into two main approaches: Adapter-based and Prompt-tuning-based. The design of the Adapter originated from [12]. It adds two adapters with residual structures in each transformer layer to fine-tune the model. During the fine-tuning process, the parameters of the original transformer are frozen, and only the parameters of the adapter layers are learned. Inspired by this, AIM [51] applied Adapter technology in action recognition. In each ViT [7] (Vision Transformer) block, AIM designed three adapters for spatial, temporal, and joint adaptation, achieving excellent results. Prompt-tuning refers to the flexible adjustment of prompts, which significantly impacts the final performance of the model. The pioneering use of prompt-tuning in the visual domain was by VPT [16]. It introduced learnable prompts within ViT while freezing the other training parameters in the network and achieved impressive results in downstream tasks related to image processing. Inspired by this, Vita-CLIP [47] designed prompt-tuning specifically for videos, which proposed the video summary tokens, frame-level prompts, and video-level prompts, achieving impressive results. Due to Adapter’s simplicity and AIM’s success in action recognition, we choose the Adapter-based method as our PEFT method.

3. Method

3.1. Problem Formulation

In the case of few-shot action recognition, the goal is to categorize an unlabeled query video into one of M action categories in the support set, with only limited K samples allotted per action class. This can be considered an M -way K -shot task. Comparable to prior research studies, we follow the episode training framework outlined by [3, 61, 56, 33, 38, 49, 46, 22, 14], where episodes are chosen randomly from a vast pool of collected data. In each episode, we assume that the set \mathcal{S} comprises $M \times K$ samples originating from M different action classes. Additionally, $S_k^m = \{s_{k1}^m, s_{k2}^m, \dots, s_{kT}^m\}$ denotes the k -th video in class $m \in \{1, \dots, M\}$ randomly sampled with T frames. Finally, the query video represents $Q = \{q_1, q_2, \dots, q_T\}$ sampled with T frames.

3.2. Architecture Overview

We choose CLIP [34] as the pre-trained foundation model, a dual-encoder structure composed of visual and text encoders. CLIP can simultaneously encode input images and texts and map them into the same vector space. It can perform cross-modal reasoning and achieve mutual conversion between images and texts. In few-shot action recognition, since there are limited labeled video samples in each task, enhancing the semanticity of videos to a great extent can be achieved by mining the semantic information of label texts and associating them with corresponding video

features. CLIP has been pre-trained on 400 million web-crawled image-text pairs, making the model highly generalizable. We choose the ViT [7] architecture in CLIP as our visual encoder. In addition, to align with textual descriptions during pre-training, input texts are usually utilized with prompt templates (the selection method of prompt templates is detailed in Sec.4.1.2). To minimize the number of trainable parameters in the model as much as possible, allowing the model to possess the ability to transfer across different tasks rapidly, we froze the pre-trained image and text encoders during fine-tuning and added some learnable lightweight adapters.

We present our overall architecture in Fig.2. For the frame-selecting strategy, we employ the approach previously used in TSN [41], which involves dividing the input video sequence into T segments and extracting snippets from each segment. We will focus on a specific scenario for simplicity and convenience: the 5-way 1-shot problem and the query set \mathcal{Q} with a single video. In this way, the query video $Q = \{q_1, q_2, \dots, q_T\}$ and the class support set videos $S^m = \{s_1^m, s_2^m, \dots, s_T^m\}$ ($S^m \in \mathcal{S} = \{S^1, S^2, \dots, S^5\}$) pass through the visual encoder (TMA) to obtain the query feature \mathbf{F}_Q and the support features \mathbf{F}_S^m ($\mathbf{F}_S^m \in \mathbf{F}_S$) in each episode. Similarly, the text descriptions C^m ($C^m \in \mathcal{C} = \{C^1, C^2, \dots, C^5\}$) pass through the text encoder to obtain text features \mathbf{F}_T^m ($\mathbf{F}_T^m \in \mathbf{F}_T$). Then we apply global average pooling operation to the features \mathbf{F}_S and \mathbf{F}_Q to obtain features \mathbf{F}_S^{avg} and \mathbf{F}_Q^{avg} . The Kullback-Leibler divergence losses \mathcal{L}_{S2T} and \mathcal{L}_{Q2T} are obtained by the cosine similarity metric between \mathbf{F}_S^{avg} , \mathbf{F}_Q^{avg} , and the text feature \mathbf{F}_T , which adapts CLIP to the few-shot action recognition task. Meanwhile, the probability distribution \mathbf{p}_{Q2T} is obtained using the cosine similarity metric. Then, features \mathbf{F}_S and \mathbf{F}_Q are passed through a text-guided prototype construction module (TPCM) with weight sharing to obtain the final features before the prototype matching process, denoted by $\widetilde{\mathbf{F}}_S$ and $\widetilde{\mathbf{F}}_Q$. Finally, the enhanced features are fed into the prototype matching metric to obtain the probability distribution \mathbf{p}_{Q2S} and loss \mathcal{L}_{Q2S} .

3.3. Task-oriented Multimodal Adaptation (TMA)

To minimize the number of tunable parameters as much as possible to avoid the overfitting phenomenon and fully leverage the spatiotemporal information in the videos and the semantic information in the texts, we propose a new method to adapt image pre-trained models for few-shot action recognition by adding lightweight adapters. The adapters we design can combine the bi-modal information of the videos and texts for task-oriented modeling.

We choose ViT [7] as our visual encoder. Specifically, consider a video clip $V \in \mathbb{R}^{T \times H \times W \times 3}$, where H, W represent the spatial size and T represents the number of frames. Each frame $t \in \{1 \dots T\}$ is divided into N non-overlapping

square patches $\{\mathbf{x}_{t,i}\}_{i=1}^N \in \mathbb{R}^{P^2 \times 3}$ of size $P \times P$, with the total number of patches being $N = HW/P^2$. Then the patches $\{\mathbf{x}_{t,i}\}_{i=1}^N \in \mathbb{R}^{P^2 \times 3}$ are then projected into the path embeddings $\mathbf{x}_{t,p} \in \mathbb{R}^{N \times D}$ through a linear projection $\mathbf{E} \in \mathbb{R}^{3P^2 \times D}$. An additional learnable [class] token $\mathbf{x}_{cls} \in \mathbb{R}^D$ to the embedded patch sequence $\mathbf{x}_{t,p}$ is presented for each frame as $\mathbf{x}_t^{(0)} = [\mathbf{x}_{cls}; \mathbf{x}_{t,p}] \in \mathbb{R}^{(N+1) \times D}$. The final per-frame token sequence fed into the ViT blocks is given by:

$$\mathbf{z}_t^{(0)} = \mathbf{x}_t^{(0)} + \mathbf{e}_{pos} \quad (1)$$

where $\mathbf{e}_{pos} \in \mathbb{R}^{(N+1) \times D}$ represents the spatial position encoding. As shown in Fig.3(b), each ViT block consists of several components, including a multihaded self-attention (MSA) mechanism, a multilayer perceptron (MLP) layer, the layer normalization (LN), and skip connections. Formally, the computation of a ViT block can be formulated as:

$$\mathbf{z}'_t^{(l)} = \mathbf{z}_t^{(l-1)} + \text{MSA} \left(\text{LN} \left(\mathbf{z}_t^{(l-1)} \right) \right) \quad (2)$$

$$\mathbf{z}_t^{(l)} = \mathbf{z}'_t^{(l)} + \text{MLP} \left(\text{LN} \left(\mathbf{z}'_t^{(l)} \right) \right) \quad (3)$$

where $\mathbf{z}_t^{(l-1)}$ and $\mathbf{z}_t^{(l)}$ represent per-frame input and the output of the l -th ViT block, respectively. And the video level representation at the l -th layer can be represented as $\mathbf{z}^{(l)} = \left[\mathbf{z}_0^{(l)} \dots \mathbf{z}_t^{(l)} \dots \mathbf{z}_T^{(l)} \right]$.

Inspired by the vision parameter-efficient fine-tuning techniques [1, 17, 16, 51, 47], we obey their ideas that keep the large pre-trained foundation model frozen to achieve robust performance while only fine-tuning a small number of extra parameters. Due to Adapter's [12] simplicity and AIM's [51] success in action recognition, we propose a task-oriented multimodal adaptation based on Adapter, which can be divided into three parts: temporal adaptation, multimodal adaptation, and joint adaptation. As shown in Fig.3(a), Adapter has a straightforward structure that includes two fully connected layers (FC), an activation layer, and a residual connection. The first FC layer maps the input to a lower dimension, while the second FC layer maps the input back to its original dimension. The support and query set branches' network structures are represented in Fig.3(c) and Fig.3(d), respectively. Since the label information of the support set data is known while that of the query set is unknown in each task, their network structures differ accordingly. Moreover, inspired by AIM [51], we reuse the pre-trained self-attention layer in the image model for temporal and multimodal adaptation to minimize the number of trainable parameters. By changing the dimensions of the input, the self-attention layer can be used in different ways. In what follows, we will introduce three types of adaptation respectively.

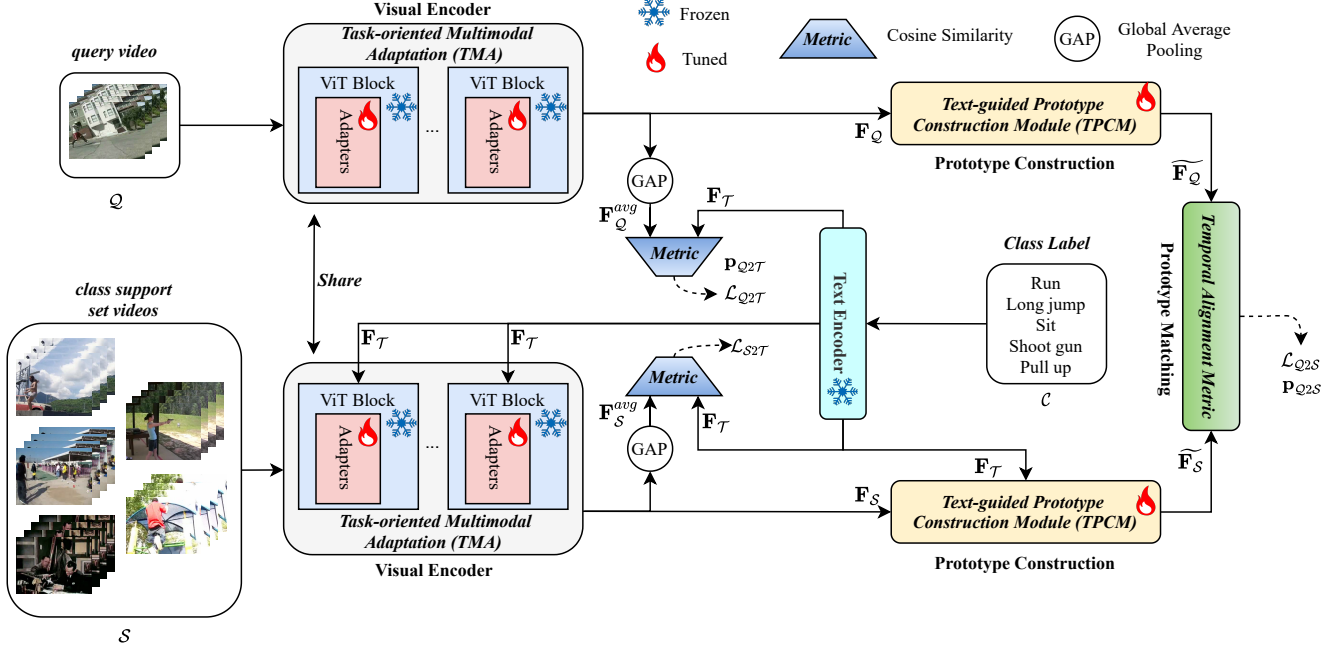


Figure 2. Overview of **MA-CLIP**. We will focus on a specific scenario for simplicity and convenience: the 5-way 1-shot problem and the query set \mathcal{Q} with a single video. The support set video features \mathbf{F}_S and query video feature \mathbf{F}_Q are obtained by the visual encoder(TMA). Similarly, text features \mathbf{F}_T are obtained using a text encoder. The text-guided prototype construction module (TPCM) generates the final features before the prototype matching process, denoted by $\widetilde{\mathbf{F}}_Q$ and $\widetilde{\mathbf{F}}_S$. The probability distribution \mathbf{p}_{Q2T} is obtained using cosine similarity metric, and \mathbf{p}_{Q2S} is calculated using prototype matching metric. The loss \mathcal{L}_{Q2S} is the standard Cross-Entropy loss and \mathcal{L}_{S2T} , \mathcal{L}_{Q2T} are Kullback-Leibler divergence (KL) loss.

3.3.1 Temporal Adaptation

Since videos have an additional temporal dimension compared to images, temporal modeling is crucial for video tasks. Based on this, we design temporal adaptation for temporal modeling. Compared to AIM, we only use the [class] token \mathbf{x}_{cls} as the input for temporal modeling, greatly reducing the computational costs. Specifically, for the l^{th} layer given the input video [class] token embedding $\mathbf{x}_{cls}^{(l-1)} \in \mathbb{R}^{T \times 1 \times D}$, we reshape it into $\mathbf{x}_{TA}^{(l-1)} \in \mathbb{R}^{1 \times T \times D}$. Then we feed $\mathbf{x}_{TA}^{(l-1)}$ into temporal adaptation to learn the temporal relationships between multiple frames, given by:

$$\mathbf{x}_{TA}^{(l)} = \mathbf{x}_{TA}^{(l-1)} + \text{Adapter} \left(\text{T-MSA} \left(\text{LN} \left(\mathbf{x}_{TA}^{(l-1)} \right) \right) \right) \quad (4)$$

where $\mathbf{x}_{TA}^{(l-1)}$ and $\mathbf{x}_{TA}^{(l)}$ denotes the temporal adaptation input and output of the l^{th} transformer block. Self-attention operates on the temporal dimension T to explore the temporal relationships between multiple frames. Inspired by AIM [51], the Adapter structure maintains the same configuration as illustrated in Fig.3(a). However, the skip connection is removed to prevent the influence of temporal adaptation during the initial training phase.

3.3.2 Multimodal Adaptation

After the temporal adaptation, we aim to integrate spatiotemporal information with text semantic information to perform multimodal adaptation to achieve task-oriented feature enhancement. Specifically, we feed the text description corresponding to the video $C^m \in \mathcal{C}$ into the text encoder to get text features \mathbf{F}_T^m ($\mathbf{F}_T^m \in \mathbf{F}_T$), which the text encoder is frozen to avoid the extra computation cost and catastrophic forgetting phenomenon. To facilitate the fusion of multimodal data, we have processed the text features $\mathbf{F}_T^m \in \mathbb{R}^{1 \times D'}$ as follows:

$$\mathbf{F}_T^{MA} = \text{Repeat} (\text{FC}_{text} (\mathbf{F}_T^m)) \quad (5)$$

where $\text{FC}_{text} \in \mathbb{R}^{D' \times D}$ aims to align text features with video features in the feature dimension, and the FC_{text} weights are shared across all layers of the visual transformer. The Repeat operation duplicates text features T times to obtain $\mathbf{F}_T^{MA} \in \mathbb{R}^{T \times 1 \times D}$. For the support set branch, given the temporal adapted features $\mathbf{x}_{TA}^{(l)} \in \mathbb{R}^{T \times 1 \times D}$, the input video features $\mathbf{z}^{(l-1)} \in \mathbb{R}^{T \times (N+1) \times D}$ and the text features $\mathbf{F}_T^{MA} \in \mathbb{R}^{T \times 1 \times D}$, we concatenate these features together along the spatial dimension to obtain the feature $\mathbf{z}_{MA-S}^{(l-1)} = [\mathbf{z}^{(l-1)}; \mathbf{x}_{TA}^{(l)}; \mathbf{F}_T^{MA}] \in \mathbb{R}^{T \times (N+3) \times D}$, where N denotes the total number of patches. However,

the corresponding text labels for the videos are unknown for the query set branch, so we can only concatenate the input video features $\mathbf{z}^{(l-1)}$ and temporal adapted features $\mathbf{x}_{TA}^{(l)}$ to obtain $\mathbf{z}_{STA-Q}^{(l-1)} = [\mathbf{z}^{(l-1)}; \mathbf{x}_{TA}^{(l)}] \in \mathbb{R}^{T \times (N+2) \times D}$.

For the support set branch, we feed $\mathbf{z}_{MA-S}^{(l-1)}$ into multimodal adaptation to integrate spatiotemporal information with text semantic information as shown in Fig.3(c), written by:

$$\mathbf{z}_{MA-S}^{(l)} = \mathbf{z}_{MA-S}^{(l-1)} + \text{Adapter} \left(\text{M-MSA} \left(\text{LN} \left(\mathbf{z}_{MA-S}^{(l-1)} \right) \right) \right) \quad (6)$$

where $\mathbf{z}_{MA-S}^{(l-1)}$ and $\mathbf{z}_{MA-S}^{(l)}$ denotes the multimodal adaptation input and output of the l^{th} transformer block. Similarly, we feed $\mathbf{z}_{MA-Q}^{(l-1)}$ into spatiotemporal adaptation to explore spatiotemporal relationships for the query set branch as shown in Fig.3(d), given by:

$$\mathbf{z}_{STA-Q}^{(l)} = \mathbf{z}_{STA-Q}^{(l-1)} + \text{Adapter} \left(\text{ST-MSA} \left(\text{LN} \left(\mathbf{z}_{STA-Q}^{(l-1)} \right) \right) \right) \quad (7)$$

where $\mathbf{z}_{STA-Q}^{(l-1)}$ and $\mathbf{z}_{STA-Q}^{(l)}$ denote the spatiotemporal adaptation input and output of the l^{th} transformer block. The Adapter's structure is the same as shown in Fig.3(b). The multimodal adaptation and spatiotemporal adaptation processes share weight parameters, allowing query and support samples to be in the same feature space. Due to the variation of videos within the same category in different tasks, the fusion of textual semantic information for that category has achieved task-oriented feature enhancement.

3.3.3 Joint Adaptation

Temporal adaptation and multimodal adaptation each have their roles, which can combine information from video-text multimodal sources for task-oriented modeling. Lastly, we introduce joint adaptation, in which an Adapter is parallel to the MLP layer to tune the final representations jointly. Specifically, to ensure the consistency of each layer of the transformer block in the spatial dimension, we perform the Select operation on $\mathbf{z}_{MA-S}^{(l)}$ and $\mathbf{z}_{STA-Q}^{(l)}$, taking the first $N+1$ features in the spatial dimension of them. Joint adaptation can be computed as follows:

$$\mathbf{z}^{(l)} = \begin{cases} \mathbf{z}_{MA-S}^{(l)} + \text{MLP} \left(\text{LN} \left(\mathbf{z}_{MA-S}^{(l)} \right) \right) + \\ \quad r \cdot \text{Adapter} \left(\text{LN} \left(\mathbf{z}_{MA-S}^{(l)} \right) \right) & \text{if } i = 0 \\ \mathbf{z}_{STA-Q}^{(l)} + \text{MLP} \left(\text{LN} \left(\mathbf{z}_{STA-Q}^{(l)} \right) \right) + \\ \quad r \cdot \text{Adapter} \left(\text{LN} \left(\mathbf{z}_{STA-Q}^{(l)} \right) \right) & \text{if } i = 1 \end{cases} \quad (8)$$

where $i = 0$ refers to the support set branch and $i = 1$ refers to the query set branch. In this context, r is a scaling factor that regulates the influence of the Adapter's output weight.

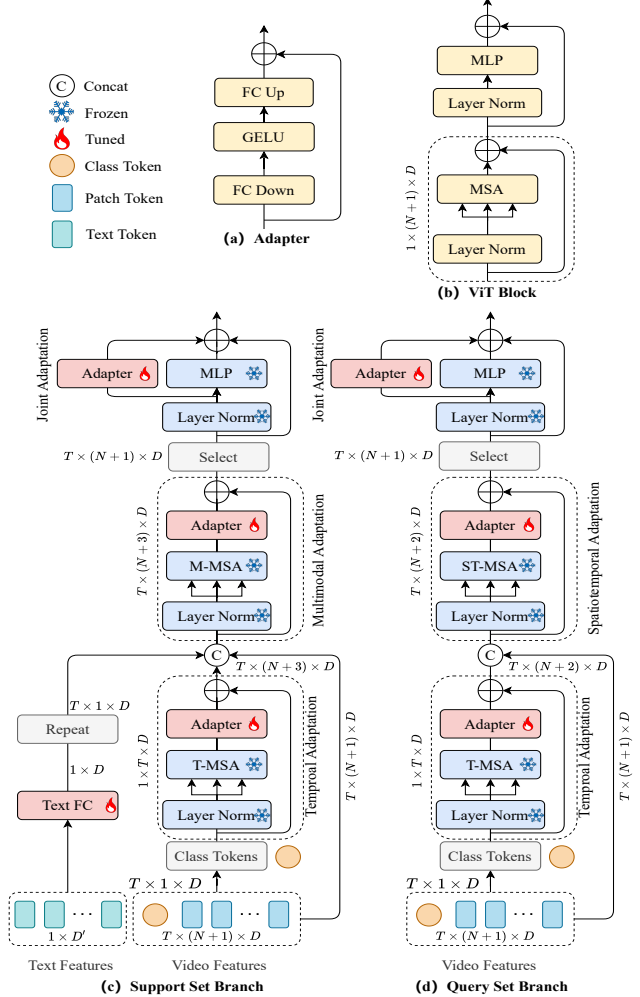


Figure 3. (a) shows the structure of the Adapter, and (b) shows the structure of a standard ViT block. (c) and (d) illustrate how we adapt the standard ViT block for the support and query set videos. Note that T-MSA, M-MSA, and ST-MSA share weights but are applied to different inputs.

3.4. Text-guided Prototype Construction Module (TPCM)

In few-shot action recognition, the quality of class prototype construction will directly affect the results of class prototype matching. The better the video class prototypes construct, the higher recognition accuracy performs, and vice versa. However, many existing methods [3, 61, 56, 33, 38, 49, 46, 22, 14] only use a limited number of videos from each category to construct class prototypes, making distinguishing similar classes in each task difficult. Recently, the success of multimodal methods in action recognition [42, 30, 18, 27, 47] has demonstrated that it is possible to understand and represent the semantic information contained in the video more accurately by jointly modeling the video data and relevant textual information. Therefore, based on the attention mechanism, we design a text-guided

prototype construction module that can fully utilize video-text information to enhance the representation of video prototypes and optimize the intra-class and inter-class correlations of videos. For the support set branch, given the support set adapted features $\mathbf{F}_S^m \in \mathbf{F}_S$ and the corresponding text features $\mathbf{F}_T^m \in \mathbf{F}_T$, we apply the cross-attention to them to obtain the enhanced features $\widetilde{\mathbf{F}}_S^m \in \widetilde{\mathbf{F}}_S$. Specifically, the query-key-value triplets $\mathbf{q}_S^m, \mathbf{k}_S^m, \mathbf{v}_S^m$ obtained process can be written as:

$$\mathbf{q}_S^m = \mathbf{F}_S^m + \text{Repeat}(\mathbf{F}_T^m) \quad (9)$$

$$\mathbf{k}_S^m = \mathbf{v}_S^m = \text{Concat}([\mathbf{F}_S^m; \mathbf{F}_T^m]) \quad (10)$$

where $\mathbf{F}_S^m \in \mathbb{R}^{T \times D'}$, $\mathbf{F}_T^m \in \mathbb{R}^{1 \times D'}$, $\mathbf{q}_S^m \in \mathbb{R}^{T \times D'}$, $\mathbf{k}_S^m = \mathbf{v}_S^m \in \mathbb{R}^{(T+1) \times D'}$, and Repeat aims to copy \mathbf{F}_T^m T times. Then, we apply the multi-head attention (MHA) and a feed-forward network to obtain the enhanced support video feature $\widetilde{\mathbf{F}}_S^m \in \mathbb{R}^{T \times D'}$ as shown in Fig.4(a), given by:

$$\widetilde{\mathbf{F}}_S^m = \mathbf{q}_S^m + \text{MHA}(\mathbf{q}_S^m, \mathbf{k}_S^m, \mathbf{v}_S^m) \quad (11)$$

$$\widetilde{\mathbf{F}}_S^m = \widetilde{\mathbf{F}}_S^m + \text{FFN}(\widetilde{\mathbf{F}}_S^m) \quad (12)$$

where MHA consists of the layer normalization and a multi-head attention layer, and FFN consists of the layer normalization and an MLP layer. Similarly, we perform the same operation on the query set videos to explore the temporal relationships, as shown in Fig.4(b). However, the difference is that $\mathbf{q}_Q^m = \mathbf{k}_Q^m = \mathbf{v}_Q^m = \mathbf{F}_Q^m \in \mathbb{R}^{T \times D'}$ since it does not have corresponding textual features. Note that the support and query set branches share the parameter weights of all modules to reduce computation costs while ensuring that query and support samples are in the same feature space.

3.5. Metric Loss and Predictions

The existing few-shot action recognition works [3, 61, 56, 33, 38, 49, 46, 22, 14], typically based solely on visual information, classify a query video by comparing the temporal-aligned distances between the query video and the support set prototypes. With the advent of text information and visual-language pre-trained model CLIP, text features can now be utilized to classify query videos. This means that query videos can be classified by matching not only with the prototypes of the support set (visual branch) but also with the corresponding text features of the support set (text branch), as shown in Fig.2. For the visual branch, given the support prototype enhanced feature $\widetilde{\mathbf{F}}_S^m \in \widetilde{\mathbf{F}}_S$ and the query enhanced feature $\widetilde{\mathbf{F}}_q \in \widetilde{\mathbf{F}}_Q$, the distance D_{q,S^m} can be calculated as:

$$D_{q,S^m} = \mathcal{M}(\widetilde{\mathbf{F}}_q, \widetilde{\mathbf{F}}_S^m) \quad (13)$$

where \mathcal{M} denotes the temporal alignment metric, and $D_{q,S^m} \in D_{q,S}$. Based on the distances $D_{q,S}$, we can obtain the probability distribution over support classes \mathbf{p}_{Q2S}

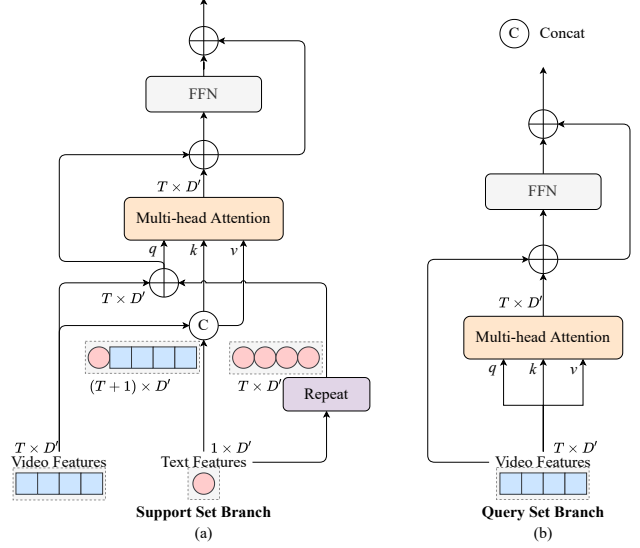


Figure 4. (a) and (b) respectively show the structure of the TPCM module for the support set and query set branch. \oplus denotes element-wise summation.

and use a standard cross-entropy loss \mathcal{L}_{Q2S} to optimize the model parameters. For the text branch, given the adapted support set prototype feature $\mathbf{F}_S^m \in \mathbf{F}_S$, adapted query feature $\mathbf{F}_q \in \mathbf{F}_Q$, and corresponding text feature $\mathbf{F}_T^m \in \mathbf{F}_T$, we apply global average pooling on temporal dimension to the features \mathbf{F}_S^m and \mathbf{F}_q to obtain \mathbf{F}_S^{m-avg} and \mathbf{F}_q^{avg} . To bring the pairwise representations of videos and labels closer to each other, we define symmetric similarities between the two modalities using cosine distances in the similarity calculation module, given by:

$$s(\mathbf{F}_S^{m-avg}, \mathbf{F}_T^m) = \frac{\langle \mathbf{F}_S^{m-avg}, \mathbf{F}_T^m \rangle}{\|\mathbf{F}_S^{m-avg}\| \|\mathbf{F}_T^m\|} \quad (14)$$

$$s(\mathbf{F}_q^{avg}, \mathbf{F}_T^m) = \frac{\langle \mathbf{F}_q^{avg}, \mathbf{F}_T^m \rangle}{\|\mathbf{F}_q^{avg}\| \|\mathbf{F}_T^m\|} \quad (15)$$

where $s(\mathbf{F}_S^{m-avg}, \mathbf{F}_T^m) \in s(\mathbf{F}_S^{avg}, \mathbf{F}_T)$ and $s(\mathbf{F}_q^{avg}, \mathbf{F}_T^m) \in s(\mathbf{F}_Q^{avg}, \mathbf{F}_T)$. Based on the cosine similarities $s(\mathbf{F}_S^{m-avg}, \mathbf{F}_T)$ and $s(\mathbf{F}_Q^{avg}, \mathbf{F}_T)$, we can obtain the softmax-normalized video-to-text similarity scores \mathbf{p}_{S2T} and \mathbf{p}_{Q2T} . Inspired by ActionCLIP [42], we define the KullbackLeibler (KL) divergence as the video-text contrastive loss \mathcal{L}_{S2T} and \mathcal{L}_{Q2T} . By optimizing contrastive loss, the CLIP model can be adapted to our downstream task. Finally, we integrate the losses of both the visual and textual branches, given by:

$$\mathcal{L} = \alpha \cdot \frac{1}{2} (\mathcal{L}_{S2T} + \mathcal{L}_{Q2T}) + (1 - \alpha) \cdot \mathcal{L}_{Q2S} \quad (16)$$

Similarly, we also combine the query set video prediction distributions from both the visual and text branches, written as:

$$\mathbf{p} = \alpha \cdot \mathbf{p}_{Q2T} + (1 - \alpha) \cdot \mathbf{p}_{Q2S} \quad (17)$$

where $\alpha \in [0, 1]$ is an adjustable hyperparameter.

4. Experiments

4.1. Experimental Setup

4.1.1 Datasets

Our method’s performance is assessed on five datasets that can be classified into two categories: 1) spatial-related datasets, including Kinetics [4], HMDB51 [20], and UCF101 [37]. 2) temporal-related datasets, including SSv2-Full [9] and SSv2-Small [9]. For spatial-related datasets, the recognition of actions primarily relies on background information, with temporal information playing a minor role. On the other hand, the situation is precisely the opposite for temporal-related datasets, where the key to action recognition lies in temporal modeling. Referring to the previous setups [3, 62, 61] on Kinetics, SSv2-Full, SSv2-Small, we select 100 classes and divide them into 64/12/24 action classes as training/validation/testing classes. For UCF101 and HMDB51, we evaluate our method on the splits provided by [56].

4.1.2 Network Architectures

We choose CLIP [34] as our pre-trained foundation model for efficient fine-tuning, where the visual encoder is ViT-B/32 [7] or ViT-B/16 [7], while the text encoder is a 12-layer, 512-wide transformer with eight attention heads. However, due to the previous works [3, 61, 56, 33, 38, 49, 46, 22, 14] that used ResNet-50 [11] pre-trained on ImageNet [5] as the backbone, we provided a version of utilizing pre-trained CLIP ResNet50 without the TMA module as our visual encoder. Meanwhile, we set the bottleneck ratio of Adapters to 0.25 in the TMA module, the same as AIM [51]. For the prompt templates of the text encoder, we follow the same approach as ActionCLIP [42]. In training, a prompt template is randomly selected from 18 candidate templates for each video. However, the vector is obtained during inference by utilizing all 18 prompt templates as inputs and taking their average. For the temporal alignment metric \mathcal{M} , we choose OTAM [3] as our baseline metric.

4.1.3 Training and Inference

Following TSN [41], we uniformly select 8 frames ($T=8$) of a video as the input augmented with some fundamental techniques, such as random horizontal flipping, cropping, and color jitter in training, while center crop in inference. For training, SSv2-Full and SSv2-Small randomly sample 100,000 training episodes, and the other datasets randomly sample 10,000 training episodes. Meanwhile, we freeze the pre-trained foundation model and only fine-tune lightweight adapters during the training process if the visual encoder is ViT-B/32 or ViT-B/16. If the visual encoder is ResNet-50, we only freeze the text encoder and fully fine-tune the visual encoder. Moreover, our framework uses the Adam

optimizer with the multi-step scheduler. As for inference, the average results of 10,000 tasks randomly sampled from the test sets in all datasets are reported in our experiments.

4.2. Results

4.2.1 Results on Spatial-related Datasets

For spatial-related datasets, the recognition of actions primarily relies on background information, with temporal modeling playing a minor role. CLIP is the large foundation image pre-trained model that mainly relies on background information to recognize images. Therefore, fine-tuning CLIP on spatial-related datasets will result in a significant improvement in few-shot action recognition. Our approach reports results using three different visual encoders. The CLIP-RN50 model has a fully fine-tuned visual encoder since it does not have an Adapter structure. On the other hand, the two ViT-B models only fine-tune lightweight adapter modules during the training process. As shown in Tab.1, even our CLIP-RN50 model significantly improves accuracy in any task setting compared to excellent methods (such as TRX [33], STRM [38], HyRSM [46], SloshNet [49], MoLo [45], et al.) that use ImageNet pre-training. Compared to CLIP-FSAR [44], which uses the same CLIP pre-training and temporal alignment metric, our MA-CLIP achieves better results in multiple datasets and task settings. Specifically, compared to CLIP-FSAR using the same ViT-B/16 as the visual encoder, our method brings 6.3%, 0.9% performance improvements in the 1-shot task of HMDB51 and Kinetics, and 0.2%, 0.6% gains in the 5-shot task of HMDB51 and Kinetics, respectively.

4.2.2 Results on Temporal-related Datasets

For temporal-related datasets, the key to action recognition is temporal information. The performance improvement from CLIP’s pre-trained weights is less significant than those for spatial-related datasets. However, our model still shows excellent results due to its remarkable capacity in temporal modeling. We report three model results using different visual encoders as shown in Tab.2. Compared to the baseline OTAM [3], our MA-CLIP using CLIP-RN50 as the visual encoder can bring 16.1%, 16.0% performance improvements in the 1-shot task, and 9.8%, 11.3% accuracy gains in the 5-shot task of SSv2-Small and SSv2-Full, respectively. Meanwhile, our CLIP-RN50 model achieves the best performance in the 1-shot task compared to all the methods using ResNet-50 as the visual encoder in all temporal-related datasets. Compared to CLIP-FSAR [44], which uses the same CLIP pre-training and temporal alignment metric, our method has a significant performance improvement. Specifically, compared to CLIP-FSAR with the same highest configuration (ViT-B/16), our MA-CLIP brings 4.5%, 2.7% accuracy improvements in the 1-shot

Table 1. State-of-the-art comparison on the 5-way k-shot benchmarks of the spatial-related benchmarks including HMDB51, SSv2, and Kinetics. The **boldface** and underline font indicate the highest and the second highest results. Note: * means our implementation. For Fine-tuning, “Full” indicates the full fine-tuning of the visual encoder, and “PEFT” indicates the parameter-efficient fine-tuning of the visual encoder.

Method	Reference	Pre-training	Fine-tuning	HMDB51		UCF101		Kinetics	
				1-shot	5-shot	1-shot	5-shot	1-shot	5-shot
MatchingNet [40]	NeurIPS(16)	INet-RN50	Full	-	-	-	-	53.3	74.6
MAML [8]	ICML(17)	INet-RN50	Full	-	-	-	-	54.2	75.3
ProtoNet [36]	NeurIPS(17)	-	Full	54.2	68.4	74.0	89.6	64.5	77.9
TRN++ [60]	ECCV(18)	INet-RN50	Full	-	-	-	-	68.4	82.0
CMN++ [61]	ECCV(18)	INet-RN50	Full	-	-	-	-	57.3	76.0
TARN [2]	BMVC(19)	-	Full	-	-	-	-	64.8	78.5
ARN [56]	ECCV(20)	-	Full	45.5	60.6	66.3	83.1	63.7	82.4
OTAM [3]	CVPR(20)	INet-RN50	Full	54.5	68.0	79.9	88.9	73.0	85.8
TTAN [24]	ArXiv(21)	INet-RN50	Full	57.1	74.0	80.9	93.2	-	-
ITANet [57]	IJCAI(21)	INet-RN50	Full	-	-	-	-	73.6	84.3
TRX [33]	CVPR(21)	INet-RN50	Full	54.9*	75.6	81.0*	96.1	65.1*	85.9
TA2N [25]	AAAI(22)	INet-RN50	Full	59.7	73.9	81.9	95.1	72.8	85.8
STRM [38]	CVPR(22)	INet-RN50	Full	57.6*	77.3	82.7*	96.9	65.1*	86.7
MTFAN [48]	CVPR(22)	INet-RN50	Full	59.0	74.6	84.8	95.1	74.6	87.4
HyRSM [46]	CVPR(22)	INet-RN50	Full	60.3	76.0	83.9	94.7	73.7	86.1
HCL [59]	ECCV(22)	INet-RN50	Full	59.1	76.3	82.5	93.9	73.7	85.8
Huang <i>etal.</i> [14]	ECCV(22)	INet-RN50	Full	60.1	77.0	71.4	91.0	73.3	86.4
Nguyen <i>etal.</i> [29]	ECCV(22)	INet-RN50	Full	59.6	76.9	84.9	95.9	74.3	87.4
SloshNet [49]	AAAI(23)	INet-RN50	Full	59.4	77.5	86.0	97.1	70.4	87.0
MoLo (OTAM) [45]	CVPR(23)	INet-RN50	Full	59.8	76.1	85.4	95.1	73.8	85.1
CLIP-FSAR [44]	ArXiv(23)	CLIP-RN50	Full	69.4	80.7	92.4	97.0	90.1	92.0
CLIP-FSAR [44]	ArXiv(23)	CLIP-ViT-B/16	Full	77.1	87.7	97.0	99.1	<u>94.8</u>	<u>95.4</u>
MA-CLIP	-	CLIP-RN50	Full	73.3	82.1	91.8	96.6	92.8	93.0
MA-CLIP	-	CLIP-ViT-B/32	PEFT	<u>77.3</u>	83.9	92.7	97.2	93.5	94.3
MA-CLIP	-	CLIP-ViT-B/16	PEFT	83.4	87.9	<u>96.5</u>	<u>98.6</u>	95.7	96.0

task, and 1.2%, 0.2% accuracy gains in the 5-shot task of SSv2-Small and SSv2-Full, respectively. For the SSv2-Small datasets, even our ViT-B/32 model can perform better than CLIP-FSAR’s ViT-B/16 model.

4.3. Ablation Study

4.3.1 Impact of The Proposed Components

To validate the contributions of each module (i.e. TMA, TPCM) in our method, we experiment under 5-way 1-shot settings on the SSv2-Small and SSv2-Full datasets. Our multimodal baseline method chooses CLIP-ViT-B/32 as our visual encoder and freezes all the learnable weights without extra modules. As shown in Tab.3, we observe each component is effective. Specifically, compared to the baseline, the TMA module can bring 13.5% and 16.3% accuracy improvements on SSv2-Small and SSv2-Full, and the TPCM module can bring 16.9% and 19.6% on two datasets. Combining all modules can get the best results, bringing 27.7% and 31.7% accuracy gains on SSv2-Small and SSv2-Full over the baseline.

4.3.2 Effectiveness of The Adaptation Components

To demonstrate the effectiveness of our proposed adaptation in TMA, we compare our method to two baselines. We choose CLIP-ViT-B/32 as our visual encoder. The first baseline is a frozen space-only model without any adaptation, freeing all the trainable parameters of the visual and text encoder but not including the TPCM module. Compared to the first baseline, the second baseline fully fine-tuned the visual encoder without any adaptation. As shown in Tab.4, the fine-tuned visual-only model can bring 12.4% performance improvement over the first baseline but the number of tunable parameters increases from 3.15M to 90.99M. Our method aims to add a few tunable parameters in a fully frozen visual model without compromising the pre-trained weights to achieve better performance than the fully fine-tuned model. In Tab.4, after multimodal adaptation, the frozen model achieves comparable performance with the full fine-tuned visual-only model (54.0 vs. 53.9) with less than one-tenth of the parameter count of the latter (7.94M vs. 90.99M). After adding temporal and joint adaptation, they bring 1.9% and 0.6% performance improve-

Table 2. State-of-the-art comparison on the 5-way k-shot benchmarks of the temporal-related benchmarks including SSv2-Small, and SSv2-Full. The **boldface** and underline font indicate the highest and the second highest results. Note: * means our implementation. For Fine-tuning, Full indicates the full fine-tuning of the visual encoder, and PEFT indicates the parameter-efficient fine-tuning of the visual encoder.

Method	Reference	Pre-training	Fine-tuning	SSv2-Small		SSv2-Full	
				1-shot	5-shot	1-shot	5-shot
MatchingNet [40]	NeurIPS(16)	INet-RN50	Full	31.3	45.5	-	-
MAML [8]	ICML(17)	INet-RN50	Full	30.9	41.9	-	-
TRN++ [60]	ECCV(18)	INet-RN50	Full	-	-	38.6	48.9
CMN++ [61]	ECCV(18)	INet-RN50	Full	34.4	43.8	36.2	48.8
OTAM [3]	CVPR(20)	INet-RN50	Full	36.4	48.0	42.8	52.3
TTAN [24]	ArXiv(21)	INet-RN50	Full	-	-	46.3	60.4
ITANet [57]	IJCAI(21)	INet-RN50	Full	39.8	53.7	49.2	62.3
TRX [33]	CVPR(21)	INet-RN50	Full	36.0*	56.7*	42.0*	64.6
TA2N [25]	AAAI(22)	INet-RN50	Full	-	-	47.6	61.0
STRM [38]	CVPR(22)	INet-RN50	Full	37.1*	55.3*	43.1*	68.1
MTFAN [48]	CVPR(22)	INet-RN50	Full	-	-	45.7	60.4
HyRSM [46]	CVPR(22)	INet-RN50	Full	40.6	56.1	54.3	69.0
HCL [59]	ECCV(22)	INet-RN50	Full	38.7	55.4	47.3	64.9
Huang <i>etal.</i> [14]	ECCV(22)	INet-RN50	Full	38.9	61.6	49.3	66.7
Nguyen <i>etal.</i> [29]	ECCV(22)	INet-RN50	Full	-	-	43.8	61.1
SloshNet [49]	AAAI(23)	INet-RN50	Full	-	-	46.5	68.3
MoLo (OTAM) [45]	CVPR(23)	INet-RN50	Full	41.9	56.2	55.0	69.6
CLIP-FSAR [44]	ArXiv(23)	CLIP-RN50	Full	52.1	55.8	58.7	62.8
CLIP-FSAR [44]	ArXiv(23)	CLIP-ViT-B/16	Full	54.6	61.8	<u>62.1</u>	<u>72.1</u>
MA-CLIP	-	CLIP-RN50	Full	52.5	57.8	58.8	63.6
MA-CLIP	-	CLIP-ViT-B/32	PEFT	<u>56.5</u>	<u>62.3</u>	61.9	64.5
MA-CLIP	-	CLIP-ViT-B/16	PEFT	59.1	64.5	63.3	72.3

Table 3. The impact of proposed modules on SSv2-Small and SSv2-Full in the 5-way 1-shot task. The visual encoder is ViT-B/32.

TMA	TPCM	SSv2-Small	SSv2-Full
✗	✗	28.8	30.2
✗	✓	42.3	46.5
✓	✗	45.7	49.8
✓	✓	56.5	61.9

ments, respectively. Our final model brings a 2.6% accuracy improvement compared to the fine-tuned visual-only model, but the number of tunable parameters is only one-fifth.

4.3.3 Comparison Between Multimodal Adaptation and Spatiotemporal Adaptation

To compare multimodal and spatiotemporal adaptation fairly, we conduct experiments on the 5-way 1-shot task of SSv2-Small and SSv2-Full. As shown in Sec.3.3.2, the difference between multimodal and spatiotemporal adaptation lies in whether or not to add text features to do self-attention with spatiotemporal features for support videos. As shown in Tab.5, using multimodal adaptation instead of spatiotemporal adaptation results in 0.6% and 0.7% performance improvements on the SSv2-Small and SSv2-Full datasets, respectively. The experimental results reveal that enhancing

the semantic representation of visual features by introducing textual features is effective in Adapter.

4.3.4 Comparison of Different Prototype Construction Methods

To demonstrate the effectiveness of our proposed module and compare the efficacy of various methods for prototype construction, we conduct the experiments on the 5-way 1-shot task of SSv2-Small. We choose CLIP-ViT-B/32 as our visual encoder, and the transformer includes the multi-head self-attention and a feed-forward network. The first baseline unimodal transformer indicates the features \mathbf{F}_S and \mathbf{F}_Q doing self-attention on the temporal dimension. The difference between the second (CLIP-FSAR[44]) and first baseline is that the text features \mathbf{F}_T are stacked along the temporal dimension before performing self-attention on the support features \mathbf{F}_S . We set all the layers of the transformer to be one. As shown in Tab.6, our TPCM module brings 8.6% and 1.8% performance improvements compared to the unimodal transformer and multimodal transformer on SSv2-Small, respectively. Based on the experimental results, our TPCM module demonstrates a higher level of efficacy in effectively leveraging textual information as guidance to integrate visual and textual features. This integration leads

Table 4. Effectiveness of the Adapter components on SSv2-Small in the 5-way 1-shot task. The visual encoder is ViT-B/32.

Method	Param (M)	Tunable Param (M)	Acc
Frozen	154.43	3.15	42.3
Fine-tuned visual-only	154.43	90.99	53.9
Frozen + multimodal adaptation	159.21	7.94	54.0
+ temporal adaptation	166.31	15.04	55.9
+ joint adaptation	169.81	18.54	56.5

Table 5. Effectiveness comparison between multimodal adaptation and spatial adaptation on SSv2-Small and SSv2-Full in the 5-way 1-shot task. The visual encoder is ViT-B/32.

Method	Dataset	Acc
Spatiotemporal Adaptation	SSv2-Small	55.9
Multimodal Adaptation	SSv2-Small	56.5
Spatiotemporal Adaptation	SSv2-Full	61.2
Multimodal Adaptation	SSv2-Full	61.9

to the attainment of more robust class prototype representations.

Table 6. Comparison of different prototype construction methods on SSv2-Small in the 5-way 1-shot task. The transformer includes the multi-head self-attention and a feed-forward network. The visual encoder is ViT-B/32.

Method	Visual Encoder	Acc
Unimodal Transformer	ViT-B/32	47.9
Multimodal Transformer	ViT-B/32	54.7
TPCM	ViT-B/32	56.5

4.3.5 Method Effectiveness on Different Temporal Alignment Metrics

We conduct the experiments using different temporal alignment metrics on the 5-way 1-shot task of Kinetics and SSv2-Small to demonstrate that our model is plug-and-play. We choose CLIP-ViT-B/32 as our visual encoder. We adopt three different temporal alignment metrics, including OTAM [3], Bi-MHM [46], and TRX [33]. As displayed in Tab.7, our method can adapt to any temporal alignment metric, and the final accuracies are closely correlated to the metric’s performance. Moreover, irrespective of the temporal alignment metric employed, our MA-CLIP consistently achieves the most outstanding performance comparing the baselines, which serves as compelling evidence for the superiority of our model.

4.3.6 Unimodal Model vs. Multimodal Model

We also compare the performance between the unimodal model and multimodal model, as well as the impacts of different pre-training. We experiment with different pre-training and model modalities on the 5-way 1-shot task of Kinetics and SSv2-Small. We conducted experiments on multiple temporally aligned metrics. We provided two baselines for each metric: an ImageNet [5] pre-trained unimodal model and a CLIP pre-trained unimodal model. We

choose ViT-B/32 as our visual encoder, and all baseline models’ visual encoders are fully fine-tuned. As shown in Tab.7, using a CLIP pre-trained single-tower model can lead to performance improvements compared to ImageNet pre-trained model, but these improvements are still relatively limited. However, when using our proposed MA-CLIP multimodal model, there is a significant improvement in performance on two datasets. Specifically, our MA-CLIP consistently achieves a minimum accuracy improvement of 15% over the unimodal model utilizing ImageNet pre-training and a minimum performance improvement of 10% over the unimodal model using CLIP pre-training on two datasets. These results, on the one hand, demonstrate the importance of text information for few-shot action recognition tasks and, on the other hand, proves the effectiveness of our approach.

4.3.7 Full Fine-tuning vs. Adaptation

In Tab.8, we conduct experiments on the 5-way 1-shot task of SSv2-Small to make a fair comparison between full fine-tuning and adaptation, which indicates the TMA module we proposed here. We choose ViT-B-32 as our visual encoder. As shown in Tab.8, our adaptation method can bring 2.6% and 2.8% accuracy improvements on SSv2-Small and SSv2-Full over the full fine-tuning model, respectively. Our adaptation method implements multimodal fusion and temporal modeling, while the full fine-tuning method does not achieve this. However, our method has only one-fifth (18.54M vs. 90.99M) of tunable parameters compared to the full fine-tuning method, requires 1.6G (11.9G vs 13.5G) less memory usage, and takes 0.4 (3.0H vs. 3.4H) hours less time to train for 10,000 tasks on a single RTX3090. The experimental results demonstrate that our MA-CLIP is fast, efficient, and has low training costs.

4.3.8 Comparison of Different Methods for The Number of Training Tasks.

To demonstrate the significance of applying large-scale foundation pre-trained models in few-shot action recognition, significantly reducing the number of training tasks and dramatically improving recognition accuracy. We conduct experiments on SSv2-Small, Kinetics in the 5-way 1-shot task to compare the number of training tasks and accuracy among different methods. The visual encoder is ViT-B/32

Table 7. Method effectiveness on different temporal alignment metrics on SSv2-Small and Kinetics in the 5-way 1-shot task. And effectiveness comparison between the unimodal model and the multimodal model. The visual encoder is ViT-B/32.

Temporal Alignment Metric	Model Modality	Pre-training	Kinetics	SSv2-Small
OTAM [3]	Unimodal	INet-ViT-B/32	75.8	38.2
OTAM [3]	Unimodal	CLIP-ViT-B/32	83.7	44.8
MA-CLIP(OTAM)	Multimodal	CLIP-ViT-B/32	93.5	56.5
Bi-MHM [46]	Unimodal	INet-ViT-B/32	75.2	39.5
Bi-MHM [46]	Unimodal	CLIP-ViT-B/32	83.2	45.5
MA-CLIP(Bi-MHM)	Multimodal	CLIP-ViT-B/32	93.2	56.9
TRX [33]	Unimodal	INet-ViT-B/32	67.2	37.3
TRX [33]	Unimodal	CLIP-ViT-B/32	82.8	42.7
MA-CLIP(TRX)	Multimodal	CLIP-ViT-B/32	92.8	52.4

Table 8. Effectiveness comparison between full fine-tuning and adaptation on SSv2-Small and SSv2-Full in the 5-way 1-shot task. The visual encoder is ViT-B/32. "Memory(G)" refers to the amount of video memory usage, and "Time(H)" indicates the time required to train 10,000 tasks, measured in hours on a single RTX3090.

Method	Dataset	Tunable Param (M)	Memory(G)	Time(H)	Acc
Full fine-tuning	SSv2-Small	90.99	13.5	3.4	53.9
Adaptation	SSv2-Small	18.54	11.9	3.0	56.5
Full fine-tuning	SSv2-Full	90.99	13.5	3.4	59.1
Adaptation	SSv2-Full	18.54	11.9	3.0	61.9

Table 9. Comparison of different methods for the number of training tasks on SSv2-Small, Kinetics in the 5-way 1-shot task. The visual encoder is ViT-B/32. MA-CLIP's temporal alignment metric is OTAM [3].

Method	Dataset	Pre-training	Num of training tasks	Acc
OTAM [3]	SSv2-Small	INet-ViT-B/32	80000	38.2
HYRSM [46]	SSv2-Small	INet-ViT-B/32	75000	40.4
TRX [33]	SSv2-Small	INet-ViT-B/32	80000	37.3
MA-CLIP	SSv2-Small	CLIP-ViT-B/32	20000	56.5
OTAM [3]	Kinetics	INet-ViT-B/32	10000	83.7
HYRSM [46]	Kinetics	INet-ViT-B/32	10000	83.2
TRX [33]	Kinetics	INet-ViT-B/32	10000	82.8
MA-CLIP	Kinetics	CLIP-ViT-B/32	1000	93.5

and MA-CLIP's temporal alignment metric is OTAM. As shown in Tab. 9, using the ViT/B-32 model, our MA-CLIP achieves at least a 15% improvement in accuracy compared to other methods that use ImageNet pre-training, while the number of training tasks is only one-fourth of theirs on SSv2-Small. Similarly, on Kinetics, our MA-CLIP achieves at least a 10% improvement in accuracy while the number of training tasks is only one-tenth of other methods. Based on the above results, applying large-scale foundation models to few-shot recognition is necessary.

4.3.9 Attention Visualization of MA-CLIP

Fig.5 shows the attention visualization of our MA-CLIP on SSv2-Small in the 5-way 1-shot setting. Corresponding to the original RGB images (left), the attention maps of the unimodal full fine-tuning model using CLIP pre-trained weights (middle), which we have mentioned in Sec.4.3.6 are compared to the attention maps with our MA-CLIP (right). As shown in Fig.5, the attention maps generated by MA-CLIP focus more on action-related objects and reduce attention to the background and unrelated objects. These

observations provide empirical evidence of the effectiveness of our MA-CLIP in enhancing semantic and spatiotemporal representation.

5. Conclusion

In this work, we propose a novel method MA-CLIP to adapt CLIP for few-shot action recognition by adding lightweight adapters, which can minimize the number of learnable parameters and enable the model to possess the ability to transfer across different tasks quickly. The adapters we designed can combine information from video-text multimodal sources for task-oriented spatiotemporal modeling, which is fast, efficient, and has low training costs. Additionally, based on the attention mechanism, we design a text-guided prototype construction module that can fully utilize video-text information to enhance the representation of video prototypes. Our MA-CLIP is plug-and-play, which can be used in any different few-shot action recognition temporal alignment metric. Experiments demonstrate that our method performs excellently using any metric in various task settings. Extensive experiments on five widely

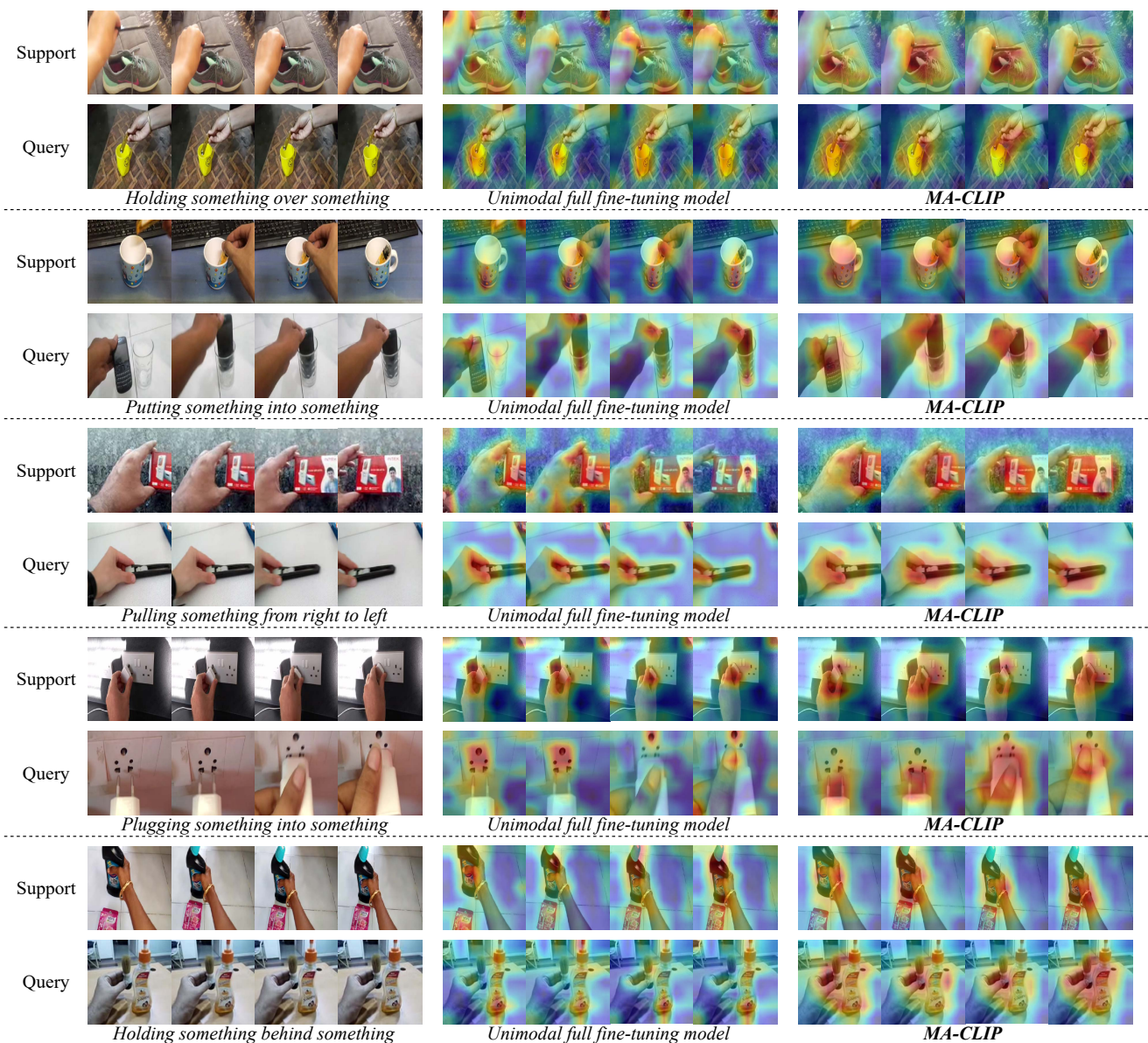


Figure 5. Attention visualization of our MA-CLIP on SSv2-Small in the 5-way 1-shot setting. Corresponding to the original RGB images(left), the attention maps of the unimodal full fine-tuning model (middle) are compared to the attention maps with our MA-CLIP (right). The temporal alignment metric is OTAM [3].

used datasets have shown that our MA-CLIP can achieve outstanding performance with minor trainable parameters.

References

- [1] Hyojin Bahng, Ali Jahanian, Swami Sankaranarayanan, and Phillip Isola. Visual prompting: Modifying pixel space to adapt pre-trained models. *arXiv preprint arXiv:2203.17274*, 2022. 2, 4
- [2] Mina Bishay, Georgios Zoupourlis, and Ioannis Patras. Tarn: Temporal attentive relation network for few-shot and zero-shot action recognition. *arXiv preprint arXiv:1907.09021*, 2019. 9
- [3] Kaidi Cao, Jingwei Ji, Zhangjie Cao, Chien-Yi Chang, and Juan Carlos Niebles. Few-shot video classification via temporal alignment. In *Proceedings of the IEEE/CVF Conference on Computer Vision and Pattern Recognition*, pages 10618–10627, 2020. 1, 3, 6, 7, 8, 9, 10, 11, 12, 13
- [4] Joao Carreira and Andrew Zisserman. Quo vadis, action recognition? a new model and the kinetics dataset. In *proceedings of the IEEE Conference on Computer Vision and Pattern Recognition*, pages 6299–6308, 2017. 8
- [5] Jia Deng, Wei Dong, Richard Socher, Li-Jia Li, Kai Li, and Li Fei-Fei. Imagenet: A large-scale hierarchical image database. In *2009 IEEE conference on computer vision and*

- pattern recognition*, pages 248–255. Ieee, 2009. 8, 11
- [6] Carl Doersch, Ankush Gupta, and Andrew Zisserman. Crosstransformers: spatially-aware few-shot transfer. *Advances in Neural Information Processing Systems*, 33:21981–21993, 2020. 3
- [7] Alexey Dosovitskiy, Lucas Beyer, Alexander Kolesnikov, Dirk Weissenborn, Xiaohua Zhai, Thomas Unterthiner, Mostafa Dehghani, Matthias Minderer, Georg Heigold, Sylvain Gelly, et al. An image is worth 16x16 words: Transformers for image recognition at scale. *arXiv preprint arXiv:2010.11929*, 2020. 3, 4, 8
- [8] Chelsea Finn, Pieter Abbeel, and Sergey Levine. Model-agnostic meta-learning for fast adaptation of deep networks. In *International conference on machine learning*, pages 1126–1135. PMLR, 2017. 2, 9, 10
- [9] Raghav Goyal, Samira Ebrahimi Kahou, Vincent Michalski, Joanna Materzynska, Susanne Westphal, Heuna Kim, Valentin Haenel, Ingo Fruend, Peter Yianilos, Moritz Mueller-Freitag, et al. The” something something” video database for learning and evaluating visual common sense. In *Proceedings of the IEEE international conference on computer vision*, pages 5842–5850, 2017. 8
- [10] Xiuye Gu, Tsung-Yi Lin, Weicheng Kuo, and Yin Cui. Open-vocabulary object detection via vision and language knowledge distillation. *arXiv preprint arXiv:2104.13921*, 2021. 2
- [11] Kaiming He, Xiangyu Zhang, Shaoqing Ren, and Jian Sun. Deep residual learning for image recognition. In *Proceedings of the IEEE conference on computer vision and pattern recognition*, pages 770–778, 2016. 8
- [12] Neil Houlsby, Andrei Giurgiu, Stanislaw Jastrzebski, Bruna Morrone, Quentin De Laroussilhe, Andrea Gesmundo, Mona Attariyan, and Sylvain Gelly. Parameter-efficient transfer learning for nlp. In *International Conference on Machine Learning*, pages 2790–2799. PMLR, 2019. 2, 3, 4
- [13] Edward J Hu, Yelong Shen, Phillip Wallis, Zeyuan Allen-Zhu, Yuanzhi Li, Shean Wang, Lu Wang, and Weizhu Chen. Lora: Low-rank adaptation of large language models. *arXiv preprint arXiv:2106.09685*, 2021. 2, 3
- [14] Yifei Huang, Lijin Yang, and Yoichi Sato. Compound prototype matching for few-shot action recognition. In *Computer Vision–ECCV 2022: 17th European Conference, Tel Aviv, Israel, October 23–27, 2022, Proceedings, Part IV*, pages 351–368. Springer, 2022. 1, 3, 6, 7, 8, 9, 10
- [15] Chao Jia, Yinfei Yang, Ye Xia, Yi-Ting Chen, Zarana Parekh, Hieu Pham, Quoc Le, Yun-Hsuan Sung, Zhen Li, and Tom Duerig. Scaling up visual and vision-language representation learning with noisy text supervision. In *International Conference on Machine Learning*, pages 4904–4916. PMLR, 2021. 1, 3
- [16] Menglin Jia, Luming Tang, Bor-Chun Chen, Claire Cardie, Serge Belongie, Bharath Hariharan, and Ser-Nam Lim. Visual prompt tuning. In *Computer Vision–ECCV 2022: 17th European Conference, Tel Aviv, Israel, October 23–27, 2022, Proceedings, Part XXXIII*, pages 709–727. Springer, 2022. 2, 3, 4
- [17] Shibo Jie and Zhi-Hong Deng. Convolutional bypasses are better vision transformer adapters. *arXiv preprint arXiv:2207.07039*, 2022. 2, 4
- [18] Chen Ju, Tengda Han, Kunhao Zheng, Ya Zhang, and Weidi Xie. Prompting visual-language models for efficient video understanding. In *Computer Vision–ECCV 2022: 17th European Conference, Tel Aviv, Israel, October 23–27, 2022, Proceedings, Part XXXV*, pages 105–124. Springer, 2022. 6
- [19] Wonjae Kim, Bokyung Son, and Ildoo Kim. Vilt: Vision-and-language transformer without convolution or region supervision. In *International Conference on Machine Learning*, pages 5583–5594. PMLR, 2021. 1, 3
- [20] Hildegard Kuehne, Hueihan Jhuang, Estibaliz Garrote, Tomaso Poggio, and Thomas Serre. Hmdb: a large video database for human motion recognition. In *2011 International conference on computer vision*, pages 2556–2563. IEEE, 2011. 8
- [21] Brian Lester, Rami Al-Rfou, and Noah Constant. The power of scale for parameter-efficient prompt tuning. *arXiv preprint arXiv:2104.08691*, 2021. 2, 3
- [22] Changzhen Li, Jie Zhang, Shuzhe Wu, Xin Jin, and Shiguang Shan. Hierarchical compositional representations for few-shot action recognition. *arXiv preprint arXiv:2208.09424*, 2022. 1, 3, 6, 7, 8
- [23] Hongyang Li, David Eigen, Samuel Dodge, Matthew Zeiler, and Xiaogang Wang. Finding task-relevant features for few-shot learning by category traversal. In *Proceedings of the IEEE/CVF conference on computer vision and pattern recognition*, pages 1–10, 2019. 3
- [24] Shuyuan Li, Huabin Liu, Rui Qian, Yuxi Li, John See, Mengjuan Fei, Xiaoyuan Yu, and Weiyao Lin. Tan: Two-stage temporal alignment network for few-shot action recognition. *arXiv preprint*, 2021. 9, 10
- [25] Shuyuan Li, Huabin Liu, Rui Qian, Yuxi Li, John See, Mengjuan Fei, Xiaoyuan Yu, and Weiyao Lin. Ta2n: Two-stage action alignment network for few-shot action recognition. In *Proceedings of the AAAI Conference on Artificial Intelligence*, volume 36, pages 1404–1411, 2022. 9, 10
- [26] Zhenguo Li, Fengwei Zhou, Fei Chen, and Hang Li. Meta-sgd: Learning to learn quickly for few-shot learning. *arXiv preprint arXiv:1707.09835*, 2017. 2
- [27] Ziyi Lin, Shijie Geng, Renrui Zhang, Peng Gao, Gerard de Melo, Xiaogang Wang, Jifeng Dai, Yu Qiao, and Hongsheng Li. Frozen clip models are efficient video learners. In *Computer Vision–ECCV 2022: 17th European Conference, Tel Aviv, Israel, October 23–27, 2022, Proceedings, Part XXXV*, pages 388–404. Springer, 2022. 6
- [28] Timo Lüddecke and Alexander Ecker. Image segmentation using text and image prompts. In *Proceedings of the IEEE/CVF Conference on Computer Vision and Pattern Recognition*, pages 7086–7096, 2022. 2
- [29] Khoi D Nguyen, Quoc-Huy Tran, Khoi Nguyen, Binh-Son Hua, and Rang Nguyen. Inductive and transductive few-shot video classification via appearance and temporal alignments. In *Computer Vision–ECCV 2022: 17th European Conference, Tel Aviv, Israel, October 23–27, 2022, Proceedings, Part XX*, pages 471–487. Springer, 2022. 9, 10

- [30] Bolin Ni, Houwen Peng, Minghao Chen, Songyang Zhang, Gaofeng Meng, Jianlong Fu, Shiming Xiang, and Haibin Ling. Expanding language-image pretrained models for general video recognition. In *Computer Vision–ECCV 2022: 17th European Conference, Tel Aviv, Israel, October 23–27, 2022, Proceedings, Part IV*, pages 1–18. Springer, 2022. [2](#), [6](#)
- [31] Alex Nichol and John Schulman. Reptile: a scalable metalearning algorithm. *arXiv preprint arXiv:1803.02999*, 2(3):4, 2018. [2](#)
- [32] Jay Patravali, Gaurav Mittal, Ye Yu, Fuxin Li, and Mei Chen. Unsupervised few-shot action recognition via action-appearance aligned meta-adaptation. In *Proceedings of the IEEE/CVF International Conference on Computer Vision*, pages 8484–8494, 2021. [3](#)
- [33] Toby Perrett, Alessandro Masullo, Tilo Burghardt, Majid Mirmehdi, and Dima Damen. Temporal-relational crosstransformers for few-shot action recognition. In *Proceedings of the IEEE/CVF Conference on Computer Vision and Pattern Recognition*, pages 475–484, 2021. [1](#), [3](#), [6](#), [7](#), [8](#), [9](#), [10](#), [11](#), [12](#)
- [34] Alec Radford, Jong Wook Kim, Chris Hallacy, Aditya Ramesh, Gabriel Goh, Sandhini Agarwal, Girish Sastry, Amanda Askell, Pamela Mishkin, Jack Clark, et al. Learning transferable visual models from natural language supervision. In *International conference on machine learning*, pages 8748–8763. PMLR, 2021. [1](#), [2](#), [3](#), [8](#)
- [35] Yongming Rao, Wenliang Zhao, Guangyi Chen, Yansong Tang, Zheng Zhu, Guan Huang, Jie Zhou, and Jiwen Lu. Densclip: Language-guided dense prediction with context-aware prompting. In *Proceedings of the IEEE/CVF Conference on Computer Vision and Pattern Recognition*, pages 18082–18091, 2022. [2](#)
- [36] Jake Snell, Kevin Swersky, and Richard Zemel. Prototypical networks for few-shot learning. *Advances in neural information processing systems*, 30, 2017. [3](#), [9](#)
- [37] Khurram Soomro, Amir Roshan Zamir, and Mubarak Shah. Ucf101: A dataset of 101 human actions classes from videos in the wild. *arXiv preprint arXiv:1212.0402*, 2012. [8](#)
- [38] Anirudh Thatipelli, Sanath Narayan, Salman Khan, Rao Muhammad Anwer, Fahad Shahbaz Khan, and Bernard Ghanem. Spatio-temporal relation modeling for few-shot action recognition. In *Proceedings of the IEEE/CVF Conference on Computer Vision and Pattern Recognition*, pages 19958–19967, 2022. [1](#), [3](#), [6](#), [7](#), [8](#), [9](#), [10](#)
- [39] Zhan Tong, Yibing Song, Jue Wang, and Limin Wang. Videomae: Masked autoencoders are data-efficient learners for self-supervised video pre-training. *arXiv preprint arXiv:2203.12602*, 2022. [1](#), [3](#)
- [40] Oriol Vinyals, Charles Blundell, Timothy Lillicrap, Daan Wierstra, et al. Matching networks for one shot learning. *Advances in neural information processing systems*, 29, 2016. [3](#), [9](#), [10](#)
- [41] Limin Wang, Yuanjun Xiong, Zhe Wang, Yu Qiao, Dahua Lin, Xiaoou Tang, and Luc Van Gool. Temporal segment networks: Towards good practices for deep action recognition. In *European conference on computer vision*, pages 20–36. Springer, 2016. [4](#), [8](#)
- [42] Mengmeng Wang, Jiazheng Xing, and Yong Liu. Actionclip: A new paradigm for video action recognition. *arXiv preprint arXiv:2109.08472*, 2021. [2](#), [6](#), [7](#), [8](#)
- [43] Wenhui Wang, Hangbo Bao, Li Dong, Johan Bjorck, Zhiliang Peng, Qiang Liu, Kriti Aggarwal, Owais Khan Mohammed, Saksham Singhal, Subhojit Som, et al. Image as a foreign language: Beit pretraining for all vision and vision-language tasks. *arXiv preprint arXiv:2208.10442*, 2022. [1](#), [3](#)
- [44] Xiang Wang, Shiwei Zhang, Jun Cen, Changxin Gao, Yingya Zhang, Deli Zhao, and Nong Sang. Clip-guided prototype modulating for few-shot action recognition. *arXiv preprint arXiv:2303.02982*, 2023. [1](#), [2](#), [3](#), [8](#), [9](#), [10](#)
- [45] Xiang Wang, Shiwei Zhang, Zhiwu Qing, Changxin Gao, Yingya Zhang, Deli Zhao, and Nong Sang. Molo: Motion-augmented long-short contrastive learning for few-shot action recognition. In *Proceedings of the IEEE/CVF Conference on Computer Vision and Pattern Recognition*, pages 18011–18021, 2023. [8](#), [9](#), [10](#)
- [46] Xiang Wang, Shiwei Zhang, Zhiwu Qing, Mingqian Tang, Zhengrong Zuo, Changxin Gao, Rong Jin, and Nong Sang. Hybrid relation guided set matching for few-shot action recognition. In *Proceedings of the IEEE/CVF Conference on Computer Vision and Pattern Recognition*, pages 19948–19957, 2022. [1](#), [3](#), [6](#), [7](#), [8](#), [9](#), [10](#), [11](#), [12](#)
- [47] Syed Talal Wasim, Muzammal Naseer, Salman Khan, Fahad Shahbaz Khan, and Mubarak Shah. Vita-clip: Video and text adaptive clip via multimodal prompting. In *Proceedings of the IEEE/CVF Conference on Computer Vision and Pattern Recognition*, pages 23034–23044, 2023. [2](#), [3](#), [4](#), [6](#)
- [48] Jiamin Wu, Tianzhu Zhang, Zhe Zhang, Feng Wu, and Yongdong Zhang. Motion-modulated temporal fragment alignment network for few-shot action recognition. In *Proceedings of the IEEE/CVF Conference on Computer Vision and Pattern Recognition*, pages 9151–9160, 2022. [9](#), [10](#)
- [49] Jiazheng Xing, Mengmeng Wang, Boyu Mu, and Yong Liu. Revisiting the spatial and temporal modeling for few-shot action recognition. *arXiv preprint arXiv:2301.07944*, 2023. [1](#), [3](#), [6](#), [7](#), [8](#), [9](#), [10](#)
- [50] Jiarui Xu, Shalini De Mello, Sifei Liu, Wonmin Byeon, Thomas Breuel, Jan Kautz, and Xiaolong Wang. Groupvit: Semantic segmentation emerges from text supervision. In *Proceedings of the IEEE/CVF Conference on Computer Vision and Pattern Recognition*, pages 18134–18144, 2022. [2](#)
- [51] Taojiannan Yang, Yi Zhu, Yusheng Xie, Aston Zhang, Chen Chen, and Mu Li. Aim: Adapting image models for efficient video action recognition. *arXiv preprint arXiv:2302.03024*, 2023. [2](#), [3](#), [4](#), [5](#), [8](#)
- [52] Han-Jia Ye, Hexiang Hu, De-Chuan Zhan, and Fei Sha. Few-shot learning via embedding adaptation with set-to-set functions. In *Proceedings of the IEEE/CVF conference on computer vision and pattern recognition*, pages 8808–8817, 2020. [3](#)
- [53] Sung Whan Yoon, Jun Seo, and Jaekyun Moon. Tapnet: Neural network augmented with task-adaptive projection for few-shot learning. In *International conference on machine learning*, pages 7115–7123. PMLR, 2019. [3](#)

- [54] Lu Yuan, Dongdong Chen, Yi-Ling Chen, Noel Codella, Xiyang Dai, Jianfeng Gao, Houdong Hu, Xuedong Huang, Boxin Li, Chunyuan Li, et al. Florence: A new foundation model for computer vision. *arXiv preprint arXiv:2111.11432*, 2021. [1](#), [3](#)
- [55] Elad Ben Zaken, Shauli Ravfogel, and Yoav Goldberg. Bitfit: Simple parameter-efficient fine-tuning for transformer-based masked language-models. *arXiv preprint arXiv:2106.10199*, 2021. [2](#), [3](#)
- [56] Hongguang Zhang, Li Zhang, Xiaojuan Qi, Hongdong Li, Philip HS Torr, and Piotr Koniusz. Few-shot action recognition with permutation-invariant attention. In *European Conference on Computer Vision*, pages 525–542. Springer, 2020. [1](#), [3](#), [6](#), [7](#), [8](#), [9](#)
- [57] Songyang Zhang, Jiale Zhou, and Xuming He. Learning implicit temporal alignment for few-shot video classification. *arXiv preprint arXiv:2105.04823*, 2021. [9](#), [10](#)
- [58] Shiyu Zhao, Zhixing Zhang, Samuel Schuster, Long Zhao, BG Vijay Kumar, Anastasis Stathopoulos, Manmohan Chandraker, and Dimitris N Metaxas. Exploiting unlabeled data with vision and language models for object detection. In *European Conference on Computer Vision*, pages 159–175. Springer, 2022. [2](#)
- [59] Sipeng Zheng, Shizhe Chen, and Qin Jin. Few-shot action recognition with hierarchical matching and contrastive learning. In *Computer Vision—ECCV 2022: 17th European Conference, Tel Aviv, Israel, October 23–27, 2022, Proceedings, Part IV*, pages 297–313. Springer, 2022. [9](#), [10](#)
- [60] Bolei Zhou, Alex Andonian, Aude Oliva, and Antonio Torralba. Temporal relational reasoning in videos. In *Proceedings of the European conference on computer vision (ECCV)*, pages 803–818, 2018. [9](#), [10](#)
- [61] Linchao Zhu and Yi Yang. Compound memory networks for few-shot video classification. In *Proceedings of the European Conference on Computer Vision (ECCV)*, pages 751–766, 2018. [1](#), [3](#), [6](#), [7](#), [8](#), [9](#), [10](#)
- [62] Zhenxi Zhu, Limin Wang, Sheng Guo, and Gangshan Wu. A closer look at few-shot video classification: a new baseline and benchmark. *arXiv preprint arXiv:2110.12358*, 2021. [8](#)